SLAC-PUB-9935

# Analysis of D0 -> K anti-K X Decays

CLEO Collaboration

*Submitted to Physical Review D*

*Stanford Linear Accelerator Center, Stanford University, Stanford, CA 94309*

Work supported by Department of Energy contract DE–AC03–76SF00515.

CLNS 96/1390 Update
CLEO 96–2
April 15, 1996

# Analysis of $D^0 \to K\bar{K}X$ Decays

D.M. Asner,[1] M. Athanas,[1] D.W. Bliss,[1] W.S. Brower,[1] G. Masek,[1] H.P. Paar,[1] J. Gronberg,[2] C.M. Korte,[2] R. Kutschke,[2] S. Menary,[2] R.J. Morrison,[2] S. Nakanishi,[2] H.N. Nelson,[2] T.K. Nelson,[2] C. Qiao,[2] J.D. Richman,[2] D. Roberts,[2] A. Ryd,[2] H. Tajima,[2] M.S. Witherell,[2] R. Balest,[3] K. Cho,[3] W.T. Ford,[3] M. Lohner,[3] H. Park,[3] P. Rankin,[3] J. Roy,[3] J.G. Smith,[3] J.P. Alexander,[4] C. Bebek,[4] B.E. Berger,[4] K. Berkelman,[4] K. Bloom,[4] D.G. Cassel,[4] H.A. Cho,[4] D.M. Coffman,[4] D.S. Crowcroft,[4] M. Dickson,[4] P.S. Drell,[4] D.J. Dumas,[4] R. Ehrlich,[4] R. Elia,[4] P. Gaidarev,[4] B. Gittelman,[4] S.W. Gray,[4] D.L. Hartill,[4] B.K. Heltsley,[4] C.D. Jones,[4] S.L. Jones,[4] J. Kandaswamy,[4] N. Katayama,[4] P.C. Kim,[4] D.L. Kreinick,[4] T. Lee,[4] Y. Liu,[4] G.S. Ludwig,[4] J. Masui,[4] J. Mevissen,[4] N.B. Mistry,[4] C.R. Ng,[4] E. Nordberg,[4] J.R. Patterson,[4] D. Peterson,[4] D. Riley,[4] A. Soffer,[4] C. Ward,[4] P. Avery,[5] C. Prescott,[5] S. Yang,[5] J. Yelton,[5] G. Brandenburg,[6] R.A. Briere,[6] T. Liu,[6] M. Saulnier,[6] R. Wilson,[6] H. Yamamoto,[6] T. E. Browder,[7] F. Li,[7] J. L. Rodriguez,[7] T. Bergfeld,[8] B.I. Eisenstein,[8] J. Ernst,[8] G.E. Gladding,[8] G.D. Gollin,[8] M. Palmer,[8] M. Selen,[8] J.J. Thaler,[8] K.W. Edwards,[9] K.W. McLean,[9] M. Ogg,[9] A. Bellerive,[10] D.I. Britton,[10] R. Janicek,[10] D.B. MacFarlane,[10] P.M. Patel,[10] B. Spaan,[10] A.J. Sadoff,[11] R. Ammar,[12] P. Baringer,[12] A. Bean,[12] D. Besson,[12] D. Coppage,[12] N. Copty,[12] R. Davis,[12] N. Hancock,[12] S. Kotov,[12] I. Kravchenko,[12] N. Kwak,[12] S.Anderson,[13] Y. Kubota,[13] M. Lattery,[13] J.K. Nelson,[13] S. Patton,[13] R. Poling,[13] T. Riehle,[13] V. Savinov,[13] M.S. Alam,[14] I.J. Kim,[14] Z. Ling,[14] A.H. Mahmood,[14] J.J. O'Neill,[14] H. Severini,[14] C.R. Sun,[14] S. Timm,[14] F. Wappler,[14] J.E. Duboscq,[15] R. Fulton,[15] D. Fujino,[15] K.K. Gan,[15] K. Honscheid,[15] H. Kagan,[15] R. Kass,[15] J. Lee,[15] M. Sung,[15] A. Undrus,[15*] C. White,[15] R. Wanke,[15] A. Wolf,[15] M.M. Zoeller,[15] X. Fu,[16] B. Nemati,[16] S.J. Richichi,[16] W.R. Ross,[16] P. Skubic,[16] M. Wood,[16] M. Bishai,[17] J. Fast,[17] E. Gerndt,[17] J.W. Hinson,[17] T. Miao,[17] D.H. Miller,[17] M. Modesitt,[17] E.I. Shibata,[17] I.P.J. Shipsey,[17] P.N. Wang,[17] M. Yurko,[17] L. Gibbons,[18] S.D. Johnson,[18] Y. Kwon,[18] S. Roberts,[18] E.H. Thorndike,[18] C.P. Jessop,[19] K. Lingel,[19] H. Marsiske,[19] M.L. Perl,[19] S.F. Schaffner,[19] R. Wang,[19] T.E. Coan,[20] J. Dominick,[20] V. Fadeyev,[20] I. Korolkov,[20] M. Lambrecht,[20] S. Sanghera,[20] V. Shelkov,[20] R. Stroynowski,[20] I. Volobouev,[20] G. Wei,[20] M. Artuso,[21] A. Efimov,[21] M. Gao,[21] M. Goldberg,[21] R. Greene,[21] D. He,[21] N. Horwitz,[21] S. Kopp,[21] G.C. Moneti,[21] R. Mountain,[21] Y. Mukhin,[21] S. Playfer,[21] T. Skwarnicki,[21] S. Stone,[21] X. Xing,[21] J. Bartelt,[22] S.E. Csorna,[22] V. Jain,[22] S. Marka,[22] A. Freyberger,[23] D. Gibaut,[23] K. Kinoshita,[23] P. Pomianowski,[23] S. Schrenk,[23] D. Cinabro,[24] B. Barish,[25] M. Chadha,[25] S. Chan,[25] G. Eigen,[25] J.S. Miller,[25] C. O'Grady,[25] M. Schmidtler,[25] J. Urheim,[25] A.J. Weinstein,[25] and F. Würthwein[25]

(CLEO Collaboration)

[1] University of California, San Diego, La Jolla, California 92093
[2] University of California, Santa Barbara, California 93106
[3] University of Colorado, Boulder, Colorado 80309-0390
[4] Cornell University, Ithaca, New York 14853
[5] University of Florida, Gainesville, Florida 32611
[6] Harvard University, Cambridge, Massachusetts 02138
[7] University of Hawaii at Manoa, Honolulu, HI 96822
[8] University of Illinois, Champaign-Urbana, Illinois, 61801
[9] Carleton University, Ottawa, Ontario K1S 5B6 and the Institute of Particle Physics, Canada
[10] McGill University, Montréal, Québec H3A 2T8 and the Institute of Particle Physics, Canada
[11] Ithaca College, Ithaca, New York 14850
[12] University of Kansas, Lawrence, Kansas 66045
[13] University of Minnesota, Minneapolis, Minnesota 55455
[14] State University of New York at Albany, Albany, New York 12222
[15] Ohio State University, Columbus, Ohio, 43210
[16] University of Oklahoma, Norman, Oklahoma 73019
[17] Purdue University, West Lafayette, Indiana 47907
[18] University of Rochester, Rochester, New York 14627
[19] Stanford Linear Accelerator Center, Stanford University, Stanford, California, 94309
[20] Southern Methodist University, Dallas, Texas 75275
[21] Syracuse University, Syracuse, New York 13244
[22] Vanderbilt University, Nashville, Tennessee 37235
[23] Virginia Polytechnic Institute and State University, Blacksburg, Virginia 24061
[24] Wayne State University, Detroit, Michigan 48202
[25] California Institute of Technology, Pasadena, California 91125

## Abstract

Using data taken with the CLEO II detector, we have studied the decays of the $D^0$ to $K^+K^-$, $K^0\bar{K}^0$, $K^0_SK^0_SK^0_S$, $K^0_SK^0_S\pi^0$, $K^+K^-\pi^0$. We present significantly improved results for $B(D^0 \to K^+K^-) = (0.454 \pm 0.028 \pm 0.035)\%$, $B(D^0 \to K^0\bar{K}^0) = (0.054 \pm 0.012 \pm 0.010)\%$ and $B(D^0 \to K^0_SK^0_SK^0_S) = (0.074 \pm 0.010 \pm 0.015)\%$ where the first errors are statistical and the second errors are the estimate of our systematic uncertainty. We also present a new upper limit $B(D^0 \to K^0_SK^0_S\pi^0) < 0.059\%$ at the 90% confidence level and the first measurement of $B(D^0 \to K^+K^-\pi^0) = (0.14 \pm 0.04)\%$.

PACS numbers: 13.25.Ft, 14.40.Lb

Typeset using REVTEX

*Permanent address: BINP, RU-630090 Novosibirsk, Russia

# I. INTRODUCTION

Detailed measurements of rare exclusive decay modes of charmed mesons provide a powerful way to probe the details of charmed decays, such as the contributions of W-exchange diagrams and final-state interactions. This allows a probe of the interplay between the weak and strong interactions. The CLEO II experiment is now reaching a level of sensitivity which allows for the systematic study of several rare decay modes of the $D^0$. In particular, we report the measurements of several decays to final states containing two or more kaons.

## A. $K^+K^-$

This decay mode is Cabibbo suppressed. Some of the Feynman diagrams leading to this final state are shown in Fig. 1. Some years ago it was observed that the ratio $B(D^0 \to K^+K^-)/B(D^0 \to \pi^+\pi^-)$ was not one. This was surprising since the two decays proceed through similar diagrams. Solutions proposed to explain the deviation from 1 include SU(3) symmetry breaking effects [1], final-state interactions [2–4], and QCD sum rules [5]. A different approach is to invoke penguin diagrams which interfere constructively with the spectator decay for $KK$ but destructively for $\pi\pi$ [6]. The results presented here can be combined with the CLEO II measurement of $D^0 \to \pi^+\pi^-$ [7] to give a better measurement of this ratio.

Table I lists a survey of theoretical predictions for the $D^0 \to K^+K^-$ branching ratio. The world average for the branching ratio is (0.454$\pm$0.029)% [11].

## B. $K^0\bar{K}^0$

The $D^0 \to K^0\bar{K}^0$ decay channel allows us to study the effect of final state interactions. The $D^0 \to K^0\bar{K}^0$ decay is expected to occur primarily via the W exchange diagrams shown in Fig. 2. Since the Cabibbo factors have opposite signs, we might expect an exact cancellation of the two amplitudes in the four-quark model. In the standard six-quark model the difference between the two amplitudes is tiny, and we thus might expect the branching fraction for the decay to be very small. However, a standard model based calculation predicts a relatively large branching fraction due to final state re-scattering, leading to a branching ratio of $B(D^0 \to K^0\bar{K}^0) = 0.3\%$ [10]. Table I gives a survey of theoretical predictions for the $D^0 \to K^0\bar{K}^0$ branching ratio. The world average for the branching ratio is (0.11$\pm$0.04)% [11].

## C. $K^0_SK^0_SK^0_S$

Since this decay was first observed by the ARGUS Collaboration ($B(D^0 \to K^0_SK^0_SK^0_S)/B(D^0 \to \bar{K}^0\pi^+\pi^-) = 0.017 \pm 0.007 \pm 0.005$) [12], there have been two other measurements, made by CLEO 1.5 ($B(D^0 \to K^0_SK^0_SK^0_S) = (0.11 \pm 0.03)\%$) [13] and by E687 ($B(D^0 \to K^0_SK^0_SK^0_S)/B(D^0 \to \bar{K}^0\pi^+\pi^-) = 0.035 \pm 0.012 \pm 0.006$) [14]. This channel is Cabibbo allowed but the decay does not proceed via a simple spectator process. Instead, its formation requires the popping of an $s\bar{s}$ pair (Fig. 3) and so its existence is an indication of either W exchange or final state interactions.

### D. $K_S^0 K_S^0 \pi^0$

There has been no previous measurement of this decay rate. This decay channel is Cabibbo-suppressed and involves the popping of $\mathrm{d\bar{d}}$ or $\mathrm{s\bar{s}}$ pairs (Fig. 4). Since the Cabibbo factors have opposite signs between the two amplitudes in each pair, we might expect an almost complete cancellation of the two amplitudes in each pair. We thus might expect the branching fraction for the decay to be very small. We do not distinguish between resonant and non-resonant decay modes. The branching ratio can be compared with that of the Cabibbo favored $K_S^0 K_S^0 K_S^0$ channel.

### E. $K^+ K^- \pi^0$

There has been no previous measurement of this decay rate. This decay is Cabibbo-suppressed (Fig. 5). We do not distinguish between resonant and non-resonant decay modes. This result can be compared with the upper limit for the doubly Cabibbo suppressed decay mode of $K^+ \pi^- \pi^0$ measured at CLEO II [15].

## II. ANALYSIS

### A. Data Sample

We use data taken with the CLEO II detector at the Cornell Electron Storage Ring between November 1990 and July 1993. The data set used in this analysis corresponds to 2.7 $\mathrm{fb}^{-1}$ of data taken on and just below the $\Upsilon(4S)$ resonance. For the statistics-limited $K^0 \bar{K}^0$ channel, we also use data collected through May 1994, corresponding to an additional 0.8 $\mathrm{fb}^{-1}$.

The CLEO II detector [16] is designed to detect both charged and neutral particles with excellent resolution and efficiency. The detector consists of a charged particle tracking system surrounded by a time-of-flight (TOF) scintillation system and an electromagnetic shower detector consisting of 7800 thallium-doped cesium iodide crystals. In the "good barrel" region, defined as the region where the angle of the shower with respect to the beam axis lies between $45^o$ and $135^o$, the r.m.s. resolution in energy is given by $\delta E/E(\%) = 0.35/E^{0.75} + 1.9 - 0.1E$ ($E$ in GeV). The tracking system, time-of-flight scintillators, and calorimeter are installed inside a 1.5 T superconducting solenoidal magnet. Immediately outside the magnet are iron and chambers for muon detection. The momentum resolution of the tracking system is given by $(\delta p/p)^2 = (0.0015p)^2 + (0.005)^2$, where $p$ is in GeV/$c$. Ionization loss information ($dE/dx$) is also provided.

### B. Procedure

We use a $D^{*+}$ tag ($D^{*+} \to D^0\pi^+$ decay mode) for all the channels except the $K^0_S K^0_S K^0_S$ channel.[1] Since this latter channel is kinematically restricted, we can see a clean signal without this tag. For the $K^0\bar{K}^0$ decay channel we add the $D^{*0}$ tag ($D^{*0} \to D^0\pi^0$ decay mode) so as to increase the number of events, even though the mass difference resolution for the $D^{*0}$ tag is not as good as that for the $D^{*+}$ tag. Table II summarizes the tags and normalization modes used. To get the Monte Carlo (MC) efficiencies, we generated 20,000 events in each channel. In this analysis, we will assume that the $D^0$ and $\bar{D}^0$ partial decay rates are equal since an inequality could only result if the processes were $CP$ violating. An earlier analysis shows that any $CP$ asymmetries are small [17]. The following analyses sum both charges.

### C. The Initial Selection

We first reconstruct the $D^0$ decay mode of interest. Details of this reconstruction can be found in the sections on each specific decay mode. The $D^0$ candidate is then combined with a pion to reconstruct a $D^{*+} \to D^0\pi^+$ candidate. This pion is denoted as the soft pion. In this reconstruction, the dominant source of background is combinatorics – random combinations of tracks which accidentally give the expected mass. This background is mostly due to either a correctly reconstructed $D^0$ which is combined with a wrong soft pion, or a fake $D^0$ in which at least one of the decay products is misidentified, combined with the correct soft pion from the $D^*$ decay.

We select $D^*$'s by requiring that the reconstructed mass difference, $\Delta M (\equiv M_{D^{*+}} - M_{D^0})$ lies within 2.0 MeV/$c^2$ ($\sim 3\sigma$) of the nominal mass difference of 145.4 MeV/$c^2$. This cut strongly suppresses the background coming from random combinations of tracks which accidentally give the expected masses.

Most of the background comes from using a wrong soft pion to form the $D^*$. We determine the number of these events by fitting the $\Delta M$ background distribution and integrating under the curve in the signal region. The functional form used is

$$a(\Delta M - m_{\pi^+})^{0.5} + b(\Delta M - m_{\pi^+})^{1.5} + c(\Delta M - m_{\pi^+})^{2.5},$$

where $m_{\pi^+}$ is $\pi^+$ mass, the first term is from a non-relativistic model of phase space, and the second and third terms are the first and second order relativistic corrections to the non-relativistic model, respectively.

The momentum spectrum for continuum charm production is peaked at large momentum, while that for the combinatoric background, from both continuum and $B$ decay, is peaked at low $D^*$ momentum. $D^*$ candidates are therefore required to have a momentum ($p$) greater than 2.45 GeV/$c$ which is equivalent to a cut of $x_p$ greater than 0.5, where $x_p = p/p_{max}$ with $p_{max} = \sqrt{E^2_{beam} - m^2_{D^*}}$. This means that we exclude charm events coming from $B$ decays.

---

[1]Throughout this paper, any reference to a specific decay or state also implies a reference to its charge conjugate.

We detect $\pi^0$'s by their decays to $\gamma\gamma$. Candidate $\pi^0$'s are formed by taking two-photon combinations. The individual photons appear as clusters in the CsI calorimeter. The energy of each cluster has to be at least 30 MeV and the di-photon combination must have at least one photon in the higher resolution portion of the calorimeter ($|\cos(\theta)| < 0.71$, where $\theta$ is the angle with respect to the beam axis). We reject all clusters matched to charged tracks in the central detector. We require that the momentum of the di-photon combination be greater than 0.2 GeV/$c$ and that the mass of this combination be within $3\sigma(\sim 15$ MeV/$c^2)$ of the nominal pion mass.

When we did a systematic check of the effects of our event selection cuts, we compared and corrected the $D^*$ momentum distribution between real data and MC using the normalization mode of $D^0 \to K^-\pi^+$ to ensure that we had the same momentum distribution for both samples. Then, we checked the effect of varying the $D^*$ momentum cut.

## III. MEASUREMENTS AND RESULTS

### A. $K^+K^-$

For this channel we apply a cut on the kaon momentum of $P_{K^\pm} > 0.3$ GeV/$c$, and require that $|\cos\theta_{\mathrm{K}^\pm}| < 0.8$ where the angle $\theta_{K^\pm}$ is the angle between the $K^\pm$ momentum in the $D^0$ rest frame and the $D^0$ laboratory momentum. Since the $D^0$, $K^+$ and $K^-$ are spinless particles, the $D^0$ decays isotropically, whereas the background shows a peak at $|\cos\theta_{\mathrm{K}^\pm}| \approx 1.0$.

Using these cuts, we obtain the $D^0$ mass spectrum shown in Fig. 6(a). For this channel the signal region is between 1.84 and 1.89 GeV/$c^2$. The $D^0$ signal region is defined to be within $3\sigma$ of the fitted mass, determined using a Gaussian fit of the real data. The number of events in the $D^0$ signal region is 2785 and the number of background events coming from the mass difference sideband region is 1119$\pm$20 where the error comes from statistics in the sideband regions, which determine the background normalization. Since we determine these numbers by scaling the $\Delta M$ sideband contributions, the error is smaller than the square root of the number of events. We also consider the statistical uncertainty in the $\Delta M$ background shape as a systematic error.

At this stage, there is the possibility that backgrounds from other charm decay modes such as $K^-\pi^+\pi^0$ are also present in the $D^0$ signal region even if most of these events lie outside it. To determine this background, we use a MC simulation of continuum charmed hadron production and decay based on JETSET 7.3, followed by a full GEANT-based simulation of the signals that the particles produce in the detector. We treat these events as data and do the $\Delta M$ sideband subtraction. The result is given in Fig. 6(a). The normalization of the simulated events is absolutely determined from the luminosity. We find 564$\pm$40 background events from this source. After subtracting all the backgrounds, we find $N(K^+K^-)$= 1102$\pm$69 for $D^0 \to K^+K^-$. In order to show how well the backgrounds are understood, the background contributions to Fig. 6(a) have been subtracted from the data (solid line) histogram and the result is shown in Fig. 6(b). This subtracted histogram was not used to calculate the yields and is included purely for illustrative purposes. For this decay mode, one advantage of the above procedure, compared with simply fitting the $K^+K^-$ mass plot, is that it avoids the necessity of fitting the complicated background shape which arises from the misidentification of other $D^0$ decay modes.

To get the branching ratio, we use $D^0 \to K^-\pi^+$ as the normalization mode

$$\frac{B(D^0 \to K^+K^-)}{B(D^0 \to K^-\pi^+)} = \left[\frac{N(K^+K^-)}{\epsilon_{K^+K^-}}\right]\left[\frac{\epsilon_{K^-\pi^+}}{N(K^-\pi^+)}\right],$$

where $N$ is the number of observed events in each case and $\epsilon$ is the corresponding reconstruction efficiency which includes the $D^{*+}$ reconstruction efficiency as determined from MC events. The detector efficiencies from MC are $\epsilon_{K^+K^-} = (22.9 \pm 0.3)\%$ and $\epsilon_{K^-\pi^+} = (37.7 \pm 0.5)\%$. We observe $N(K^-\pi^+) = 15633 \pm 202$ for $D^0 \to K^-\pi^+$. We measure $B(D^0 \to K^+K^-)/B(D^0 \to K^-\pi^+) = 0.116 \pm 0.007$.

As a systematic check of the effect of our event selection cuts, we extract the signal yields with the mass difference cut, $D^*$ momentum cut and the decay angle cut individually tightened by 20% of their nominal values. We take the largest effect on the yield as setting the size of the systematic error, giving a contribution to the systematic error of 2.0%. The systematic error, due to the statistical uncertainty in the $\Delta M$ background functional form used to get the number of background events coming from the mass difference sideband region, is 5.3%. The variations of the yield with different sideband subtractions and different fitting methods are negligible compared to the other systematic errors. The systematic error due to limited MC statistics is 2.0%. This gives a total systematic error of 6.0%. Using $B(D^0 \to K^-\pi^+) = (3.91 \pm 0.08 \pm 0.17)\%$ [18], we measure $B(D^0 \to K^+K^-) = (0.454 \pm 0.028 \pm 0.035)\%$.

### B. $K^0\bar{K}^0$

We study the $K^0_SK^0_S$ component of this decay. Due to the small number of events, we use both the $D^{*\pm}$ tag and the $D^{*0}$ tag.

In this channel the dominant sources of backgrounds are from non-resonant $K^0_S\pi^+\pi^-$ and $\pi^+\pi^-\pi^+\pi^-$ production. To reduce feed-through from $D^0 \to K^0_S\pi^+\pi^-$, where the $\pi^+\pi^-$ fakes a $K^0_S$ or from $D^0 \to \pi^+\pi^-\pi^+\pi^-$, where the four pions fake 2 $K^0_S$'s, we first reconstruct $K^0_S$ mesons from $\pi^+\pi^-$ pairs with an invariant mass within 0.0108 GeV/$c^2$($\sim 3\sigma$) of the nominal $K^0_S$ mass and a vertex displaced at least 5 mm from the beam position. We also apply a $|\cos_{\theta_{K^0_S}}| < 0.8$ cut, where the angle $\theta_{K^0_S}$ is the angle between the $K^0_S$ momentum in the $D^0$ rest frame and the $D^0$ laboratory momentum.

To get the branching ratio, we use

$$\frac{B(D^0 \to K^0\bar{K}^0)}{B(D^0 \to \bar{K}^0\pi^+\pi^-)} = \frac{1}{B(K^0_S \to \pi^+\pi^-)}\left[\frac{N(K^0_SK^0_S)}{\epsilon_{K^0_SK^0_S}}\right]\left[\frac{\epsilon_{K^0_S\pi^+\pi^-}}{N(K^0_S\pi^+\pi^-)}\right],$$

where $N$ is the number of observed events in each case and $\epsilon$ is the corresponding reconstruction efficiency. Because $B(D^0 \to K^0\bar{K}^0) = 2B(D^0 \to K^0_SK^0_S)$ ($D^0 \to K^0_SK^0_L$ is forbidden) [19], the factors $B(\bar{K}^0\pi^+\pi^- \to K^0_S\pi^+\pi^-)$ and $B(K^0\bar{K}^0 \to K^0_SK^0_S)$ become equal and cancel in the above equation [20]. We use $B(K^0_S \to \pi^+\pi^-) = (68.6 \pm 0.3)\%$ [11]. The yield was extracted in the same way as for the $K^+K^-$ channel.

### 1. $D^{*\pm}$ tag

Using the $D^{*\pm}$ tag, we obtain the $D^0$ mass spectrum shown in Fig. 7(a). For this tag the signal region is between 1.84 and 1.89 GeV/$c^2$. The number of events in the $D^0$ signal region is 21 and the number of background events coming from the mass difference sideband region is 2.8±0.8, yielding $N(K_S^0 K_S^0) = 18.2 \pm 4.6$. At this stage, in order to check the background from other charm decay modes, we run on Monte Carlo events using the same cuts as for the $K^0\bar{K}^0$ channel. We find that the background comes from the non-resonant $\pi^+\pi^-$ decay modes such as $K_S^0\pi^+\pi^-$ and $\pi^+\pi^-\pi^+\pi^-$ and therefore is calculated using the sideband method. Since real data is more reliable and has a smaller associated statistical error than the Monte Carlo events, we use only the real data for background subtraction and use the sideband region of the $K_S^0$ mass domain to determine the non-resonant $\pi^+\pi^-$ background. We consider this background to be a source of a systematic error. The detection efficiencies determined by MC are $\epsilon_{K_S^0 K_S^0} = (8.4 \pm 0.2)\%$ and $\epsilon_{K_S^0\pi^+\pi^-} = (13.4 \pm 0.3)\%$. We get $N(K_S^0\pi^+\pi^-) = 4470 \pm 137$, giving $B(D^0 \to K^0\bar{K}^0)/B(D^0 \to \bar{K}^0\pi^+\pi^-) = 0.0094 \pm 0.0024$ for this tag.

### 2. $D^{*0}$ tag

We use a more restrictive mass difference cut $|M_{D^{*0}} - M_{D^0} - 0.1423| < 0.0022$ GeV/$c^2$ ($\sim 2.5\sigma$) for the $D^{*0}$ tag since the resolution of the mass difference is poorer for this channel. We obtain the $D^0$ mass spectrum shown in Fig. 7(b). For this tag the signal region lies between 1.84 and 1.89 GeV/$c^2$. The number of events in the $D^0$ signal region is 11 and the number of background events coming from the mass difference sideband region is 3.4±0.8. This gives $N(K_S^0 K_S^0) = 7.6 \pm 3.4$ after background subtraction. The detection efficiencies determined from MC are $\epsilon_{K_S^0 K_S^0} = (3.5 \pm 0.2)\%$ and $\epsilon_{K_S^0\pi^+\pi^-} = (6.8 \pm 0.6)\%$. We get $N(K_S^0\pi^+\pi^-) = 1589 \pm 71$, and we measure $B(D^0 \to K^0\bar{K}^0)/B(D^0 \to \bar{K}^0\pi^+\pi^-) = 0.0134 \pm 0.0060$ for this tag.

Fig. 7(c) shows the sum of the $D^{*\pm}$ tag and the $D^{*0}$ tag data after subtracting all the backgrounds. As a systematic check of the effect of our event selection cuts, we extract the signal yields with the mass difference cut, $D^*$ momentum cut, the decay angle cut, the vertex cut and the $K_S^0$ mass cut individually tightened by 20% of their nominal values. We take the largest effect on the yield as setting the size of the systematic error. Another systematic error is due to the possibility that backgrounds from other charm decay modes such as $\bar{K}^0\pi^+\pi^-$ or $\pi^+\pi^-\pi^+\pi^-$ are also present in the $D^0$ signal region. In order to check this, we studied a sideband region in the $K_S^0$'s mass domain to determine the non-resonant $\pi^+\pi^-$ background. Results indicate that there are 0.7 non-resonant $\pi^+\pi^-$ background events in $D^0$ signal region for the $D^{*\pm}$ tag and none for the $D^{*0}$ tag. The other systematic error is the uncertainty in the $K_S^0$ finding efficiency. This error on this efficiency is 5% per $K_S^0$, which gives a correlated systematic error affecting both $D^{*\pm}$ and $D^{*0}$ tags. All the other systematic errors are uncorrelated. A summary of the systematic errors for this channel is given in Table III.

The final ratios of $B(D^0 \to K^0\bar{K}^0)/B(D^0 \to \bar{K}^0\pi^+\pi^-)$ are $0.0094 \pm 0.0024 \pm 0.0017 \pm 0.0005$ for the $D^{*\pm}$ tag and $0.0134 \pm 0.0060 \pm 0.0021 \pm 0.0007$ for the $D^{*0}$ tag where the first errors are statistical, the second are the uncorrelated systematic errors and the last are the correlated systematic errors. Finally, we combine the data from the two tags. The combined ratio is $B(D^0 \to K^0\bar{K}^0)/B(D^0 \to \bar{K}^0\pi^+\pi^-) = 0.0101 \pm 0.0022(stat) \pm 0.0016(sys)$. Using $B(D^0 \to \bar{K}^0\pi^+\pi^-) = (5.3 \pm 0.6)\%$ [11], we obtain $B(D^0 \to K^0\bar{K}^0) = (0.054 \pm 0.012(stat) \pm 0.010(sys))\%$.

### C. $K^0_S K^0_S K^0_S$

This particular mode is essentially background free due to its kinematics, so we do not require a $D^*$ tag. Three $K^0_S$'s have to be observed, which makes the efficiency rather low, so the $K^0_S$ cuts used for this decay are looser than those we use for the other analyses described in this paper.

We first reconstruct $K^0_S$ mesons from $\pi^+\pi^-$ pairs with an invariant mass within 0.0108 GeV/$c^2$($\sim 3\sigma$) of the nominal $K^0_S$ mass and a vertex displaced at least 2 mm from the beam position. We plot the $K^0_S K^0_S K^0_S$ invariant mass for $P_{D^0} > 2.48$ GeV/$c$ which is similar to requiring $x_p$ greater than 0.5. For this mode, we have to use the fitting method. We do not use a $D^{*+}$ tag and therefore we do not do a mass difference sideband subtraction. This $K^0_S K^0_S K^0_S$ invariant mass distribution is fitted using a Gaussian and Chebyshev polynomial of order 1. We obtain a signal of $N(K^0_S K^0_S K^0_S) = 61.0 \pm 8.4$ (Fig. 8).

To get the branching ratio, we use

$$\frac{B(D^0 \to K^0_S K^0_S K^0_S)}{B(D^0 \to \bar{K}^0\pi^+\pi^-)} = \frac{1}{B(K^0_S \to \pi^+\pi^-)^2}\left[\frac{N(K^0_S K^0_S K^0_S)}{\epsilon_{K^0_S K^0_S K^0_S}}\right]\left[\frac{\epsilon_{K^0_S\pi^+\pi^-}}{2N(K^0_S\pi^+\pi^-)}\right],$$

where $N$ is the number of observed events in each case and $\epsilon$ is the corresponding reconstruction efficiency. The detection efficiencies determined from MC are $\epsilon_{K^0_S K^0_S K^0_S} = (5.2 \pm 0.2)\%$ and $\epsilon_{K^0_S\pi^+\pi^-} = (16.8 \pm 0.4)\%$. We get $N(K^0_S\pi^+\pi^-) = 14993 \pm 457$. Using $B(K^0_S \to \pi^+\pi^-) = (68.6 \pm 0.3)\%$ [11], we measure $B(D^0 \to K^0_S K^0_S K^0_S)/B(D^0 \to \bar{K}^0\pi^+\pi^-) = 0.0139 \pm 0.0019$.

As a systematic check, we study the variations of the yield with the $D^0$ momentum cut, the vertex cut and the $K^0_S$ mass cut individually tightened by 20% of their nominal values. The biggest systematic error due to these cut variations is 13.5%. The systematic error due to the $K^0_S$ finding efficiency for two $K^0_S$ in the CLEO II detector is 10.0%. The systematic error due to the MC statistics is 3.9%. So, the total systematic error is 17.2%. Finally, using $B(D^0 \to \bar{K}^0\pi^+\pi^-) = (5.3 \pm 0.6)\%$ [11], we measure $B(D^0 \to K^0_S K^0_S K^0_S) = (0.074 \pm 0.010(stat) \pm 0.015(sys))\%$.

### D. $K^0_S K^0_S \pi^0$

In this decay mode, there are very few events and the background is large. So, we use the same tight cuts on the $K^0_S$'s as we do for the $K^0_S K^0_S$ channel.

For this channel the signal region is between 1.82 and 1.90 GeV/$c^2$. The number of events in the signal region is 35 and the number of background events, estimated using the mass difference sidebands, is 24±2. Using the same methods as for the $K^+K^-$ channel, we find from Monte Carlo that other charm decay modes contribute 6±6 events to the signal region. After subtracting all the backgrounds (Fig. 9), we get $N(K_S^0 K_S^0 \pi^0) = 5 \pm 9$. The corresponding un-subtracted figures are omitted. The signal is consistent with zero. We therefore calculate an upper limit on the branching fraction.

To get the branching ratio, we use

$$\frac{B(D^0 \to K_S^0 K_S^0 \pi^0)}{B(D^0 \to \bar{K}^0 \pi^+ \pi^-)} = \frac{1}{B(K_S^0 \to \pi^+ \pi^-)} \left[ \frac{N(K_S^0 K_S^0 \pi^0)}{\epsilon_{K_S^0 K_S^0 \pi^0}} \right] \left[ \frac{\epsilon_{K_S^0 \pi^+ \pi^-}}{2N(K_S^0 \pi^+ \pi^-)} \right],$$

where $N$ is the number of the observed events in each case and $\epsilon$ is the corresponding reconstruction efficiency. The detection efficiencies determined from MC are $\epsilon_{K_S^0 K_S^0 \pi^0} = (5.3 \pm 0.2)\%$ and $\epsilon_{K_S^0 \pi^+ \pi^-} = (13.4 \pm 0.3)\%$. All the systematic errors are negligible given the size of the statistical error and so have not been included. We get $N(K_S^0 \pi^+ \pi^-) = 3184 \pm 102$. Using $B(K_S^0 \to \pi^+ \pi^-) = (68.6 \pm 0.3)\%$, we get $B(D^0 \to K_S^0 K_S^0 \pi^0)/B(D^0 \to \bar{K}^0 \pi^+ \pi^-) = 0.0029 \pm 0.0052$. Using $B(D^0 \to \bar{K}^0 \pi^+ \pi^-) = (5.3 \pm 0.6)\%$ [11], we measure $B(D^0 \to K_S^0 K_S^0 \pi^0) = (0.015 \pm 0.027)\%$ or $B(D^0 \to K_S^0 K_S^0 \pi^0) < 0.059\%$ at the 90% confidence level.

### E. $K^+ K^- \pi^0$

Finally, we measure $D^0 \to K^+ K^- \pi^0$. For this decay mode, the misidentification of a $\pi^+$ as a $K^+$ is the largest source of background. The major source of this background is from the decay $D^{*+} \to D^0 \pi^+$ followed by the Cabibbo favored decay $D^0 \to K^- \pi^+ \pi^0$. Since the branching ratio $B(D^0 \to K^- \pi^+ \pi^0)$ for this background is much bigger than the branching ratio $B(D^0 \to K^- \pi^+)$ for the $K^+ K^-$ channel background ($B(D^0 \to K^- \pi^+ \pi^0)/B(D^0 \to K^- \pi^+) = 3.78 \pm 0.071$ [21]), we use tighter cuts than those for the $K^+ K^-$ channel.

In order to select the $K^+ K^- \pi^0$ decay mode and reduce the $K^- \pi^+ \pi^0$ background, we change a kaon candidate track assignment to a pion candidate track and calculate the resultant $D^0$ mass ($M_{K^- \pi^+ \pi^0}$). If $M_{K^- \pi^+ \pi^0}$ is within $3\sigma$ of the nominal $D^0$ mass, we eliminate the combination. We also use a tight cut $P_{D^{*+}} > 2.93$ GeV/$c$ which is equivalent to requiring $x_p$ greater than 0.6.

We require that the normalized difference between the expected and measured $dE/dx$ for the kaon hypothesis be within $2\sigma$ for both kaons. We also require $P_{K^\pm} > 0.3$ GeV/$c$. We use the same $\pi^0$ selection described in section II C except for requiring that the momentum of the $\pi^0$ be greater than 0.4 GeV/$c$ and that the mass of the $\pi^0$ be within $2\sigma(\sim 10\text{MeV}/c^2)$ of the nominal pion mass.

Using these cuts, we obtain the $D^0$ mass spectrum shown in Fig. 10 after doing the normalized mass difference sideband subtraction. For this mode, we have to use the fitting method since the backgrounds from other charm decay modes are so complicated that the fitting method is more reliable. It is fitted by a Gaussian and a Chebyshev polynomial of order 2. We get a signal of $N(K^+ K^- \pi^0) = 151 \pm 42$, and $\epsilon_{K^+ K^- \pi^0} = (9.2 \pm 0.3)\%$.

To get the branching ratio, we use

$$\frac{B(D^0 \to K^+ K^- \pi^0)}{B(D^0 \to K^- \pi^+ \pi^0)} = \left[ \frac{N(K^+ K^- \pi^0)}{\epsilon_{K^+ K^- \pi^0}} \right] \left[ \frac{\epsilon_{K^- \pi^+ \pi^0}}{N(K^- \pi^+ \pi^0)} \right].$$

We get $\epsilon_{K^- \pi^+ \pi^0} = (4.7 \pm 0.3)\%$ and $N(K^- \pi^+ \pi^0) = 8151 \pm 246$, giving the ratio $B(D^0 \to K^+ K^- \pi^0)/B(D^0 \to K^- \pi^+ \pi^0) = 0.0095 \pm 0.0026$. Using the ratio $B(D^0 \to$

$K^-\pi^+\pi^0)/B(D^0 \to K^-\pi^+) = 3.78 \pm 0.071$ [21] and $B(D^0 \to K^-\pi^+) = (3.91 \pm 0.08 \pm 0.17)\%$ [18], we get $B(D^0 \to K^+K^-\pi^0) = (0.14 \pm 0.04)\%$. All the other systematic errors are negligible given the size of the statistical error.

## IV. SUMMARY AND CONCLUSIONS

We have investigated $D^0$ decays to several rare final states which have two or three kaons in the final state. Figures 11, 12 and 13 show the previous measurements and our results for $K^+K^-$, $K^0\bar{K}^0$ and $K^0_S K^0_S K^0_S$ respectively. Table IV gives the final summary of our results, where the first error is statistical and the second is the estimate of our systematic uncertainty. The $K^+K^-$, $K^0\bar{K}^0$ and $K^0_S K^0_S K^0_S$ results have significantly smaller errors than earlier measurements. We also report the first upper limit on the $D^0 \to K^0_S K^0_S \pi^0$ branching fraction and the first measurement of the $D^0 \to K^+K^-\pi^0$ branching fraction.


## ACKNOWLEDGEMENTS

We gratefully acknowledge the efforts of the CESR staff in providing us with excellent luminosity and running conditions. J.P.A., J.R.P., and I.P.J.S. thank the NYI program of the NSF, M.S thanks the PFF program of the NSF, G.E. thanks the Heisenberg Foundation, K.K.G., M.S., H.N.N., T.S., and H.Y. thank the OJI program of DOE, J.R.P, K.H., and M.S. thank the A.P. Sloan Foundation, and A.W., and R.W. thank the Alexander von Humboldt Stiftung for support. This work was supported by the National Science Foundation, the U.S. Department of Energy, and the Natural Sciences and Engineering Research Council of Canada.

# REFERENCES


[1] M. Bauer *et al.*, Z. Phys. C **34**, 103 (1987).
[2] L. L. Chau, Phys. Rep. **95**, 1 (1983).
[3] A. N. Kamal *et al.*, Phys. Rev. D **35**, 3515 (1987); D **36**, 3510 (1987); L. L. Chau *et al.*, Phys. Lett. B **280**, 281 (1992).
[4] A. Czarnecki *et al.*, Z. Phys. C **54**, 411 (1992).
[5] B. Yu and M. Shifman, Sov. J. Nucl. Phys. **45**, 522 (1987).
[6] M. Gluck, Phys. Lett. B **88**, 145 (1979); J. Finjord, Nucl. Phys. B **181**, 74 (1981).
[7] CLEO Collaboration, M. Selen *et al.*, Phys. Rev. Lett. **71**, 1973 (1993).
[8] N. Cabibbo and L. Maiani, Phys. Lett. B **73**, 418 (1978).
[9] I. I. Bigi, Nucl. Phys. B **281**, 41 (1987).
[10] X. Y. Pham, Phys. Lett. B **193**, 331 (1987).
[11] Particle Data Group, Phys. Rev. D **50**, 1173 (1994).
[12] ARGUS Collaboration, H. Albrecht *et al.*, Z. Phys. C **46**, 9 (1990).
[13] CLEO Collaboration, R. Ammar *et al.*, Phys. Rev. D **44**, 3383 (1991).
[14] E687 Collaboration, P. L. Frabetti *et al.*, Phys. Lett. B **340**, 254 (1994).
[15] CLEO Collaboration, G. Crawford *et al.*, ICHEP94, Ref. GLS0458 (1994).
[16] CLEO Collaboration, Y. Kubota *et al.*, Nucl. Instrum. Methods Phys. Res., Sect. A **320**, 66 (1992).
[17] CLEO Collaboration, J. Bartelt *et al.*, Phys. Rev. D **52**, 4860 (1995).
[18] CLEO Collaboration, D. S. Akerib *et al.*, Phys. Rev. Lett. **71**, 3070 (1993).
[19] This factor could differ from two if other diagrams contributed to the decay and interfered. $CP$ violation allows for the possibility that the $D^0$ can decay to $K_S^0 K_L^0$. However, we assume that any such contributions would be small and can safely be neglected.
[20] CLEO Collaboration, J. Alexander *et al.*, Phys. Rev. Lett. **65**, 1184 (1990).
[21] CLEO Collaboration, L. Gibbons *et al.*, EPS0179, CLEO CONF95-18 (1995).
[22] MARK2 Collaboration, G. S. Abrams *et al.*, Phys. Rev. Lett. **43**, 481 (1979).
[23] MARK3 Collaboration, R. M. Baltrusaitis *et al.*, Phys. Rev. Lett. **55**, 150 (1985).
[24] E691 Collaboration, J. C. Anjos *et al.*, Phys. Rev. D **44**, R3371 (1991).
[25] NA14 Collaboration, M. P. Alvarez *et al.*, Z. Phys. C **50**, 11 (1991).
[26] E687 Collaboration, P. L. Frabetti *et al.*, Phys. Lett. B **281**, 167 (1992).
[27] OMEGA Collaboration, M. Adamovich *et al.*, Phys. Lett. B **280**, 163 (1992).
[28] E687 Collaboration, P. L. Frabetti *et al.*, Phys. Lett. B **321**, 295 (1994).
[29] E400 Collaboration, J. P. Cumalat *et al.*, Phys Lett. B **210**, 253 (1988).

FIGURES

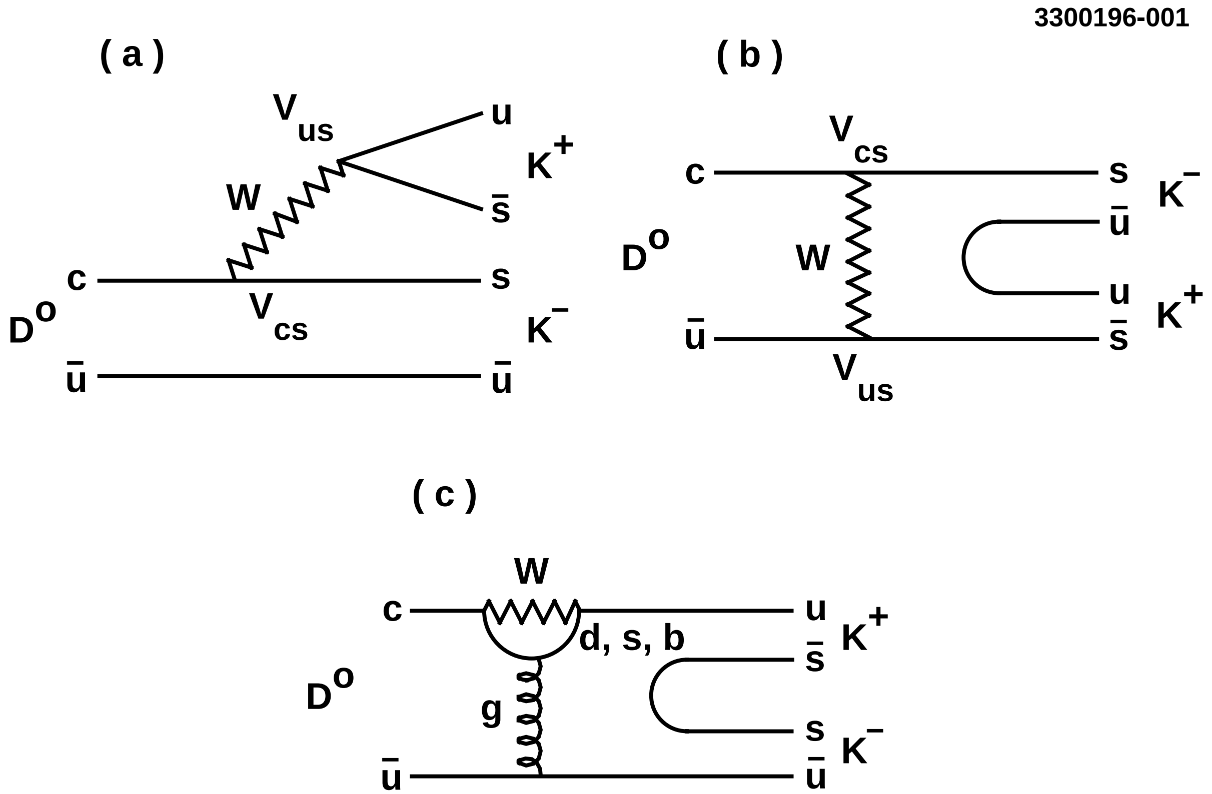


FIG. 1. The most important Feynman diagrams for $D^0 \to K^+K^-$: (a) quark decay, (b) W exchange decay and (c) penguins.

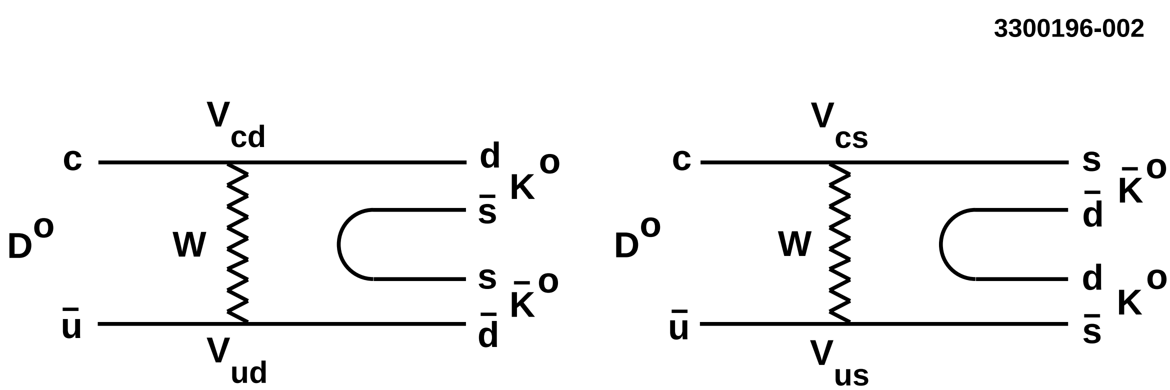


FIG. 2. The Feynman diagrams for $D^0 \to K^0\bar{K}^0$.

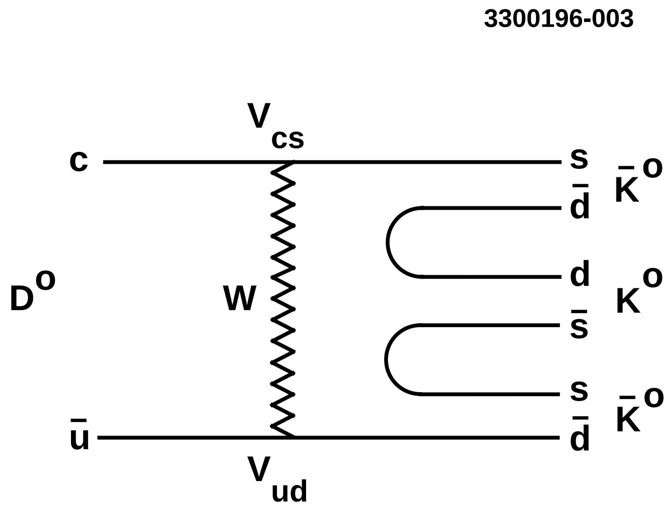


FIG. 3. The Feynman diagram for $D^0 \to K^0_S K^0_S K^0_S$.

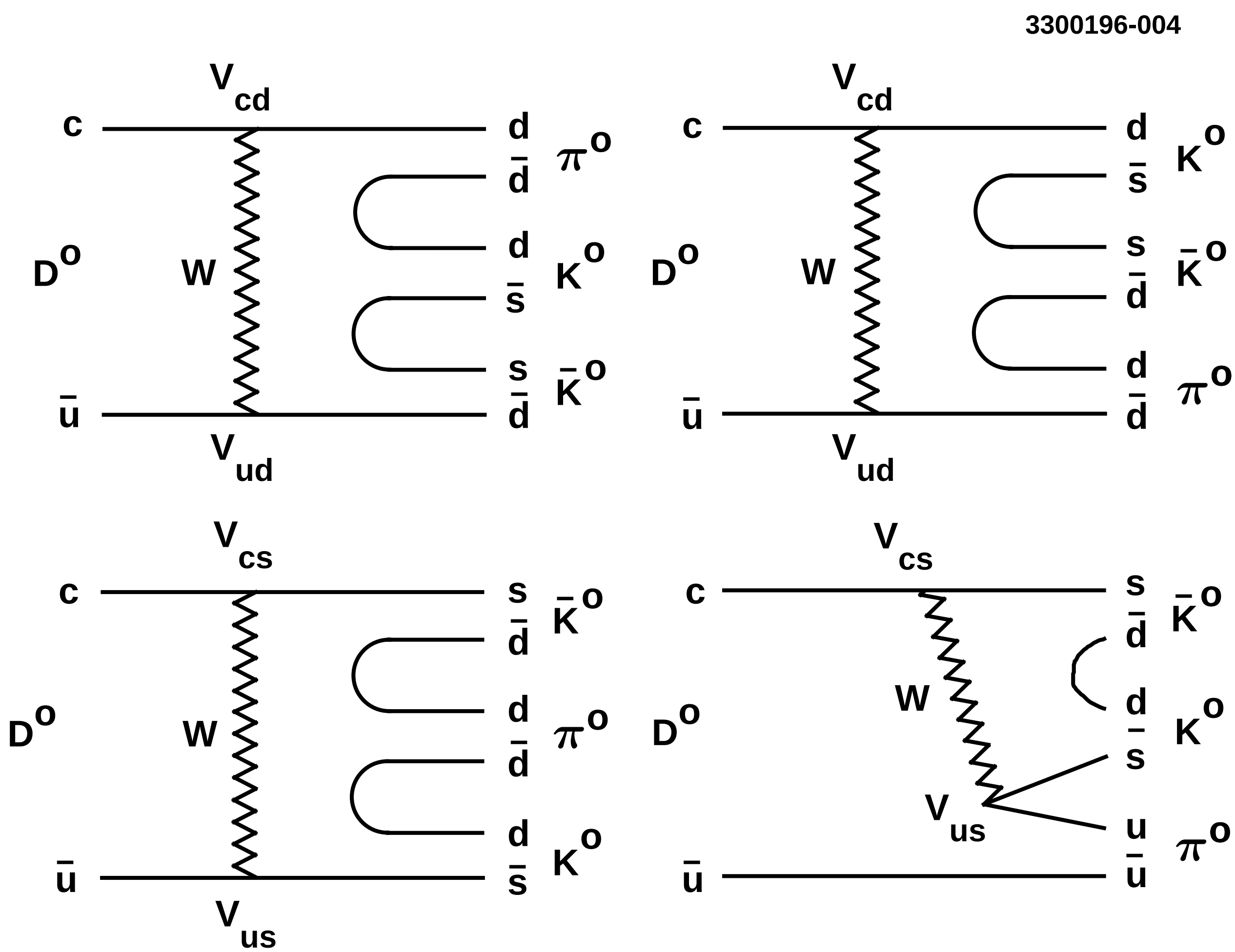


FIG. 4. The most important Feynman diagrams for $D^0 \to K^0_S K^0_S \pi^0$.

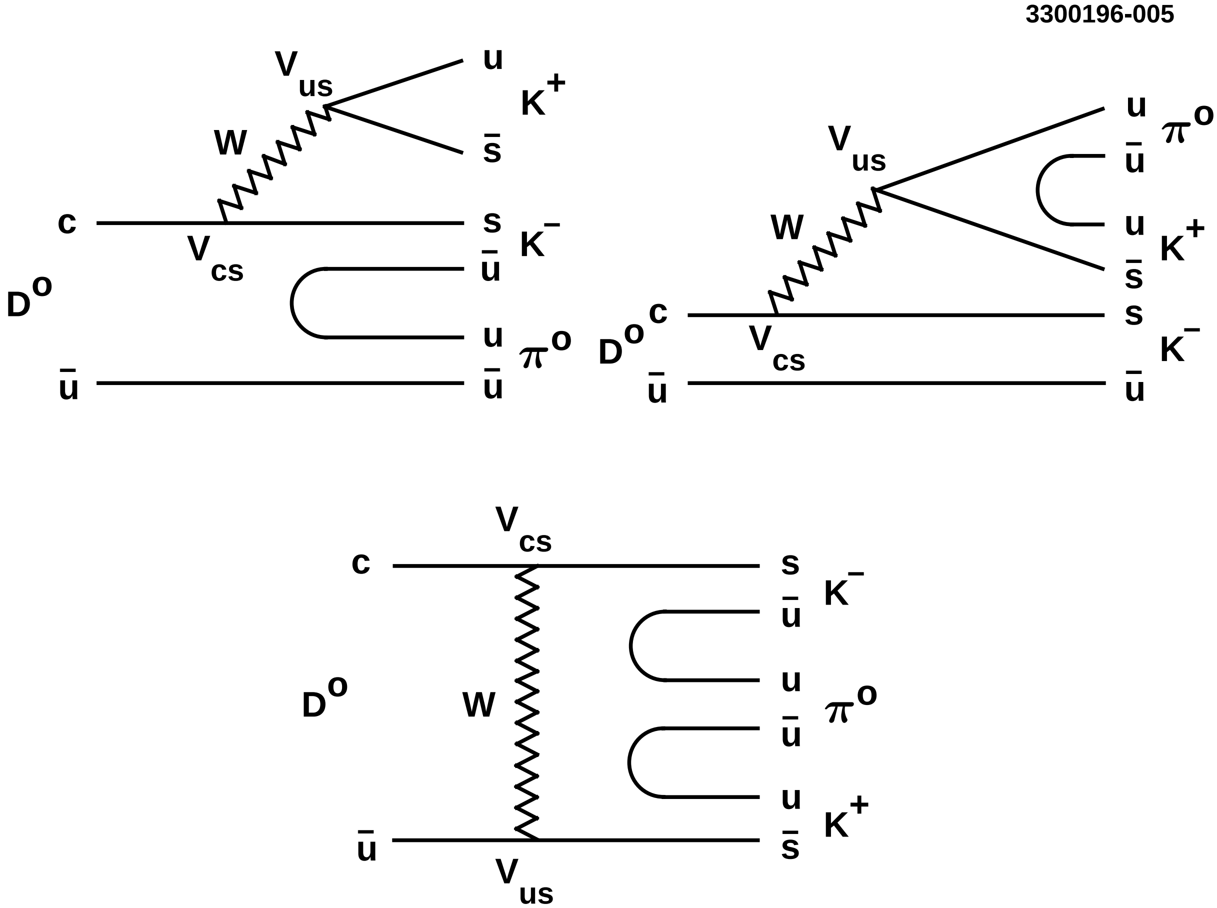


FIG. 5. The most important Feynman diagrams for $D^0 \to K^+K^-\pi^0$.

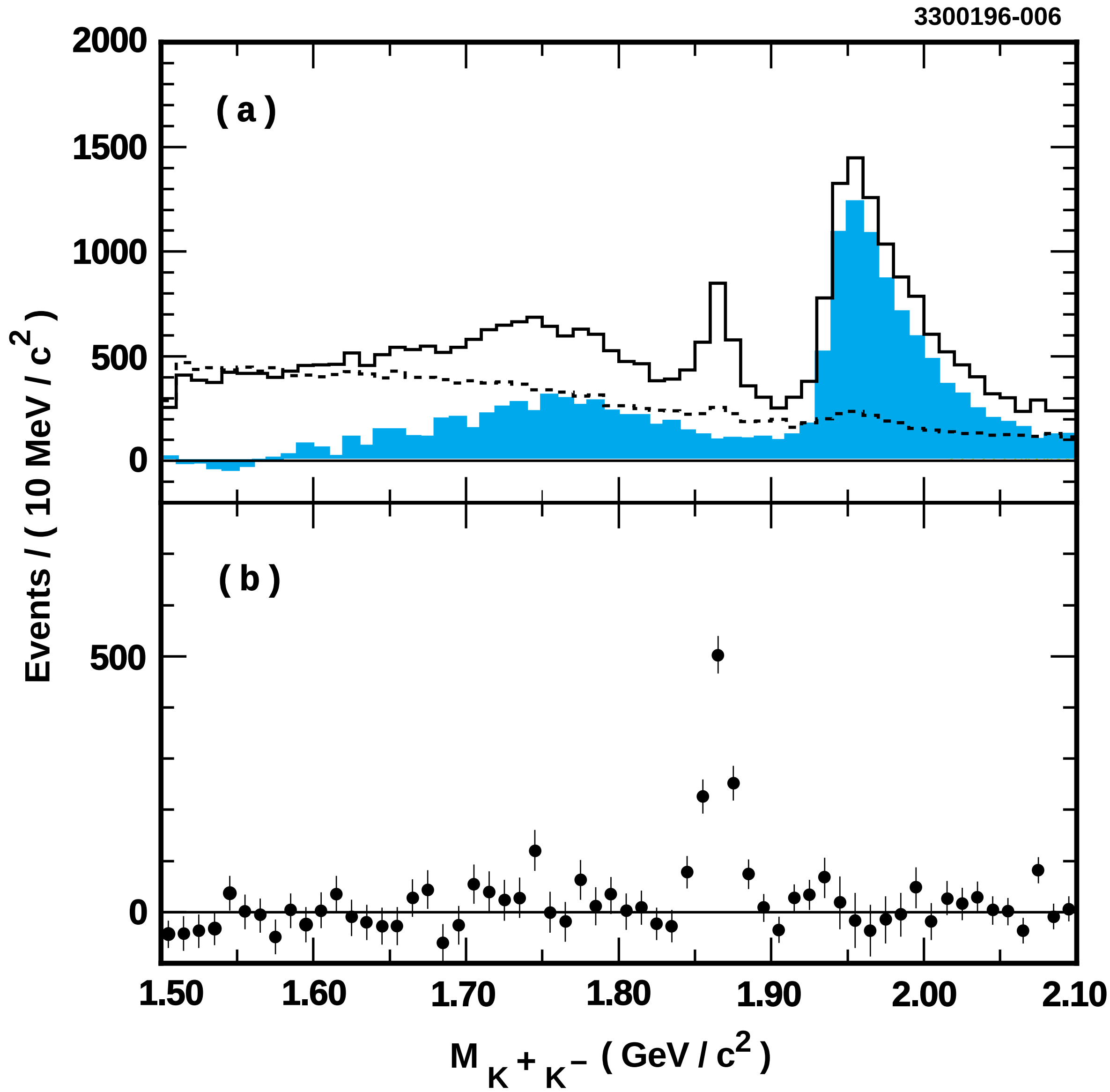


FIG. 6. (a) The $K^+K^-$ invariant mass distribution. The solid line is the $D^0$ mass signal in the mass difference signal region. The dotted line is background from the mass difference sideband region. The shaded area represents the background coming from other charm decay modes after doing the $\Delta M$ sideband subtraction. This background is determined by Monte Carlo events. We see a peak around 1.98 GeV/$c^2$ due to misidentified $D^0 \to K^-\pi^+$ events. (b) The reconstructed $K^+K^-$ invariant mass distribution after subtracting all the backgrounds.

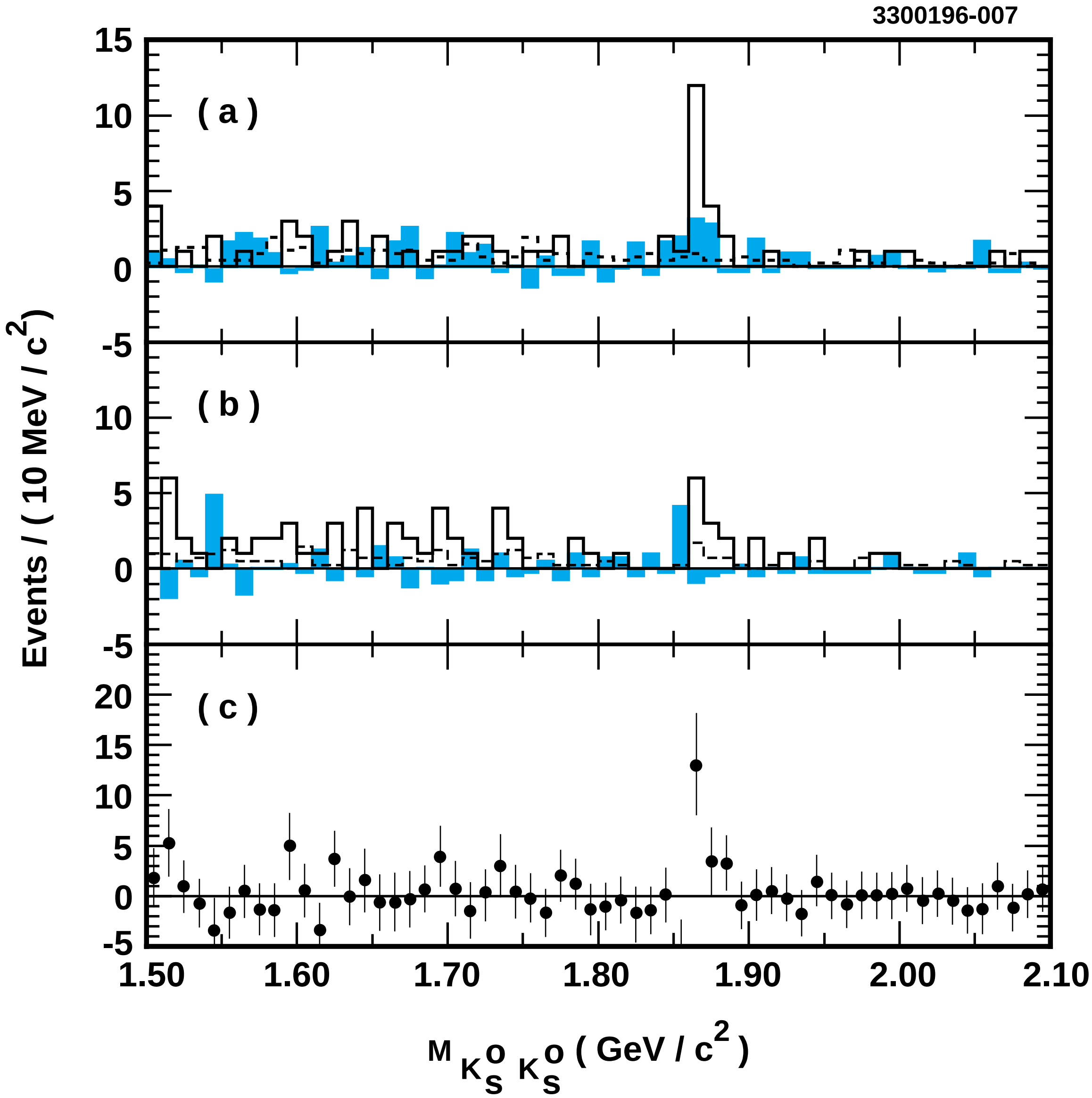


FIG. 7. (a) The invariant mass distribution for $K_S^0 K_S^0$ for the $D^{*\pm}$ tag. (b) The invariant mass distribution for $K_S^0 K_S^0$ for the $D^{*0}$ tag. The solid line is the $D^0$ mass signal in the mass difference signal region. The dotted line is background from the mass difference sideband region. The shaded area represents the background coming from other charm decay modes after doing the mass difference sideband subtraction. This background is determined by Monte Carlo events. (c) The sum of the invariant mass distribution for $K_S^0 K_S^0$ for $D^{*\pm}$ tag and $D^{*0}$ tag data after subtracting all the backgrounds.

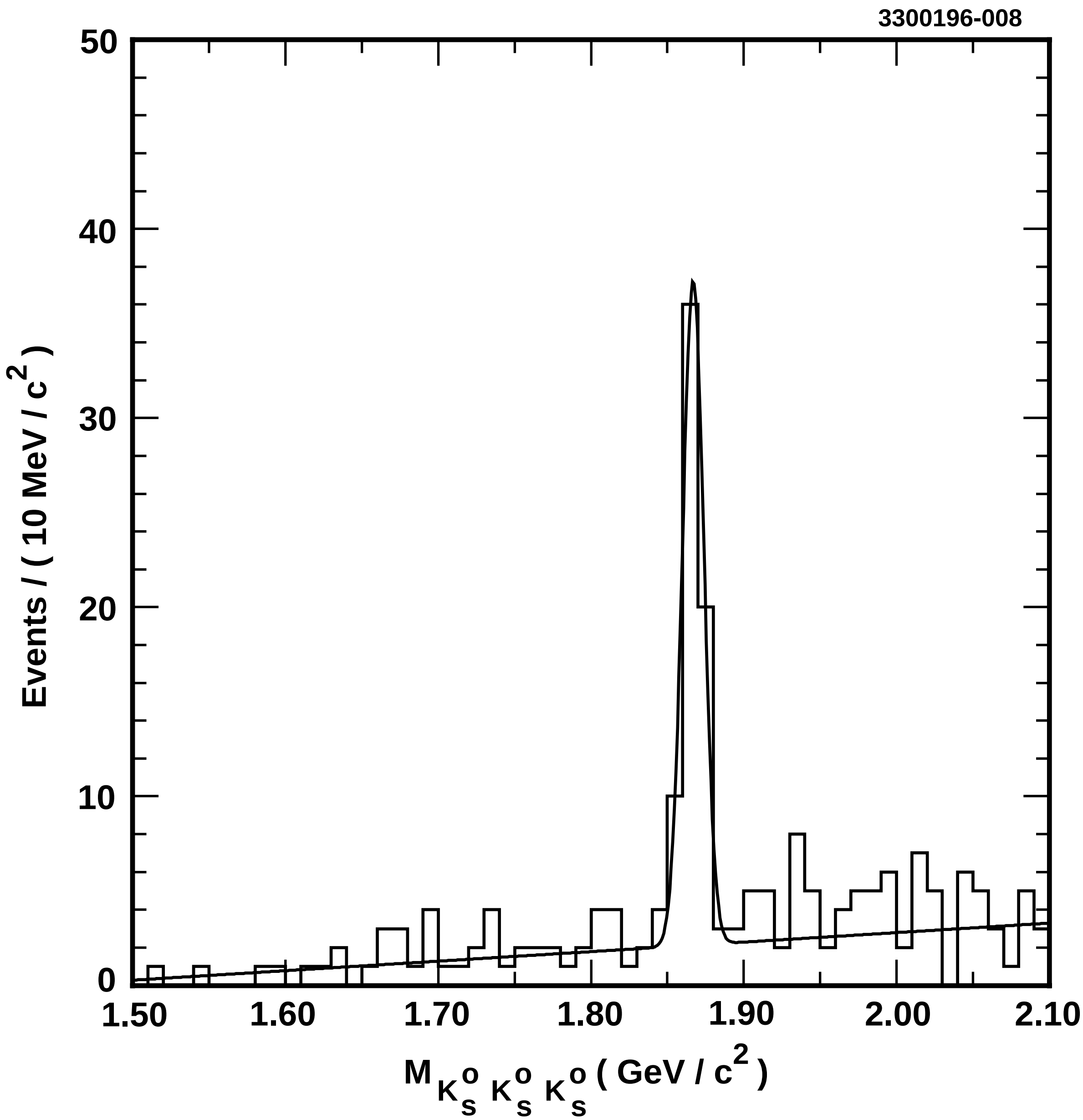


FIG. 8. The invariant mass distribution of $K_S^0 K_S^0 K_S^0$. The signal is fitted using a Gaussian while the background is fit to a straight line.

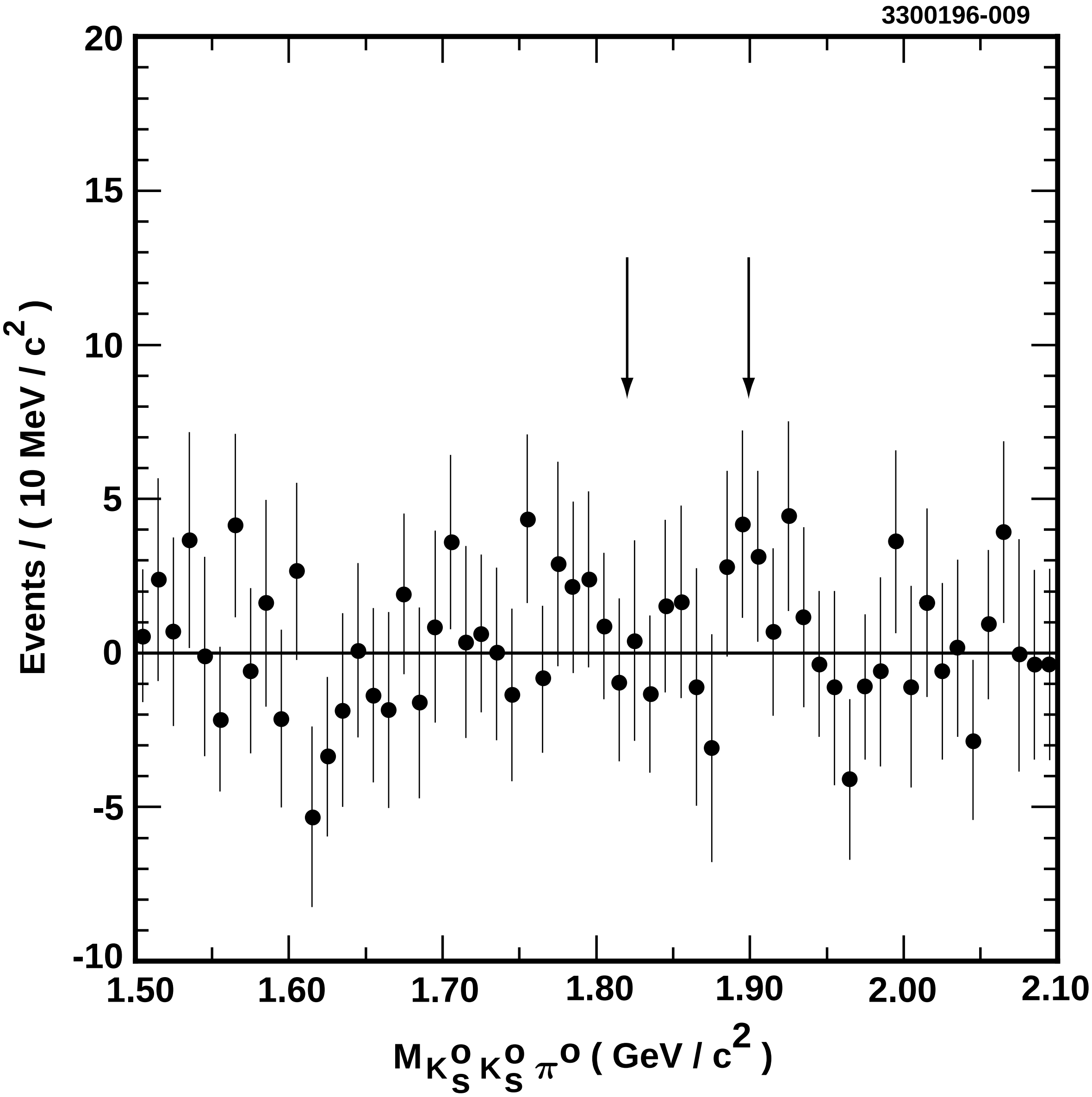


FIG. 9. The invariant mass distribution of $K_S^0 K_S^0 \pi^0$ after subtracting all the backgrounds. The arrows show the signal region.

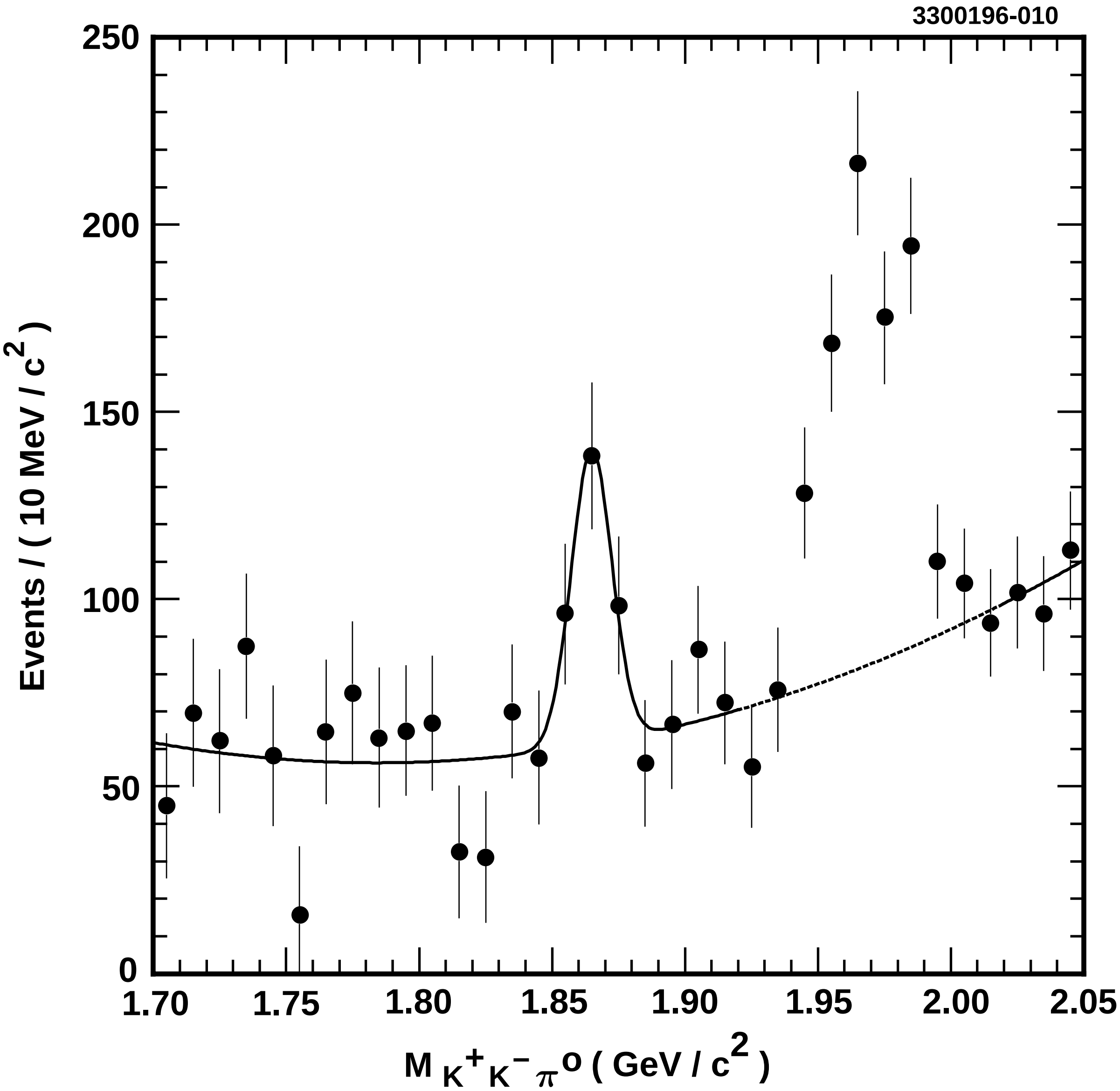


FIG. 10. The invariant mass distribution of $K^+K^-\pi^0$ after doing the normalized mass difference sideband subtraction. In fitting, we exclude the region between 1.92 and 2.02 GeV/$c^2$ due to an excess of misidentified $D^0 \to K^-\pi^+\pi^0$ events which survive the veto.

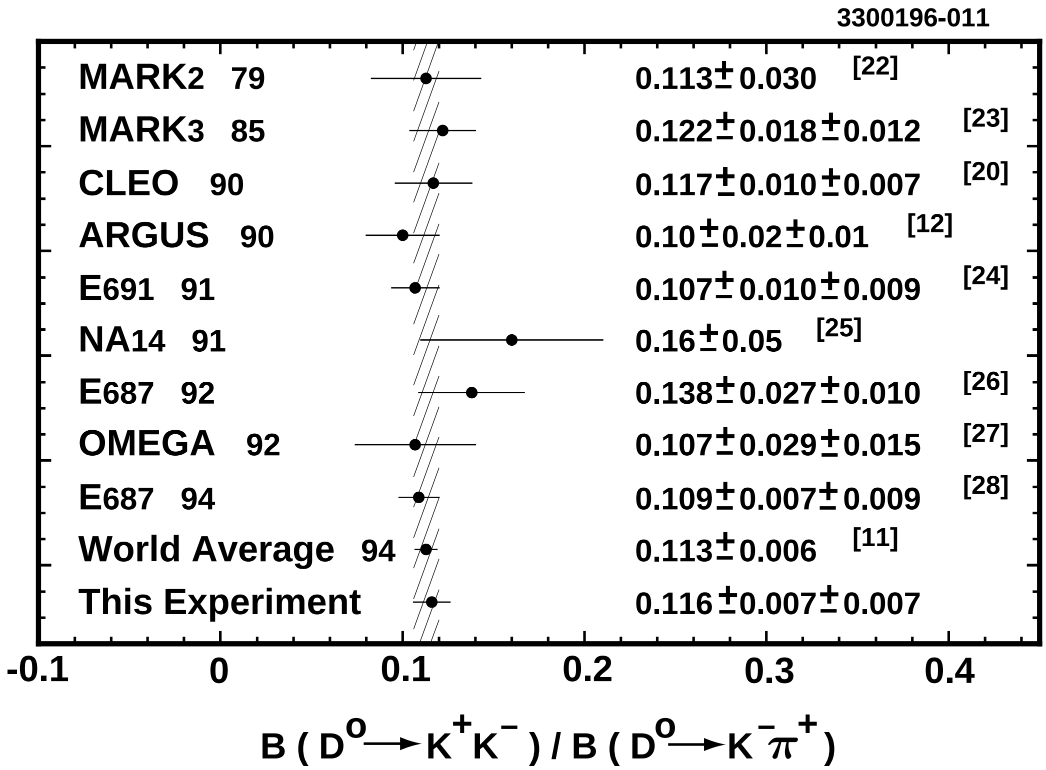


FIG. 11. The previous measurements and our result for the $B(D^0 \to K^+K^-)/B(D^0 \to K^-\pi^+)$ ratio. The hatched area indicates the world average.

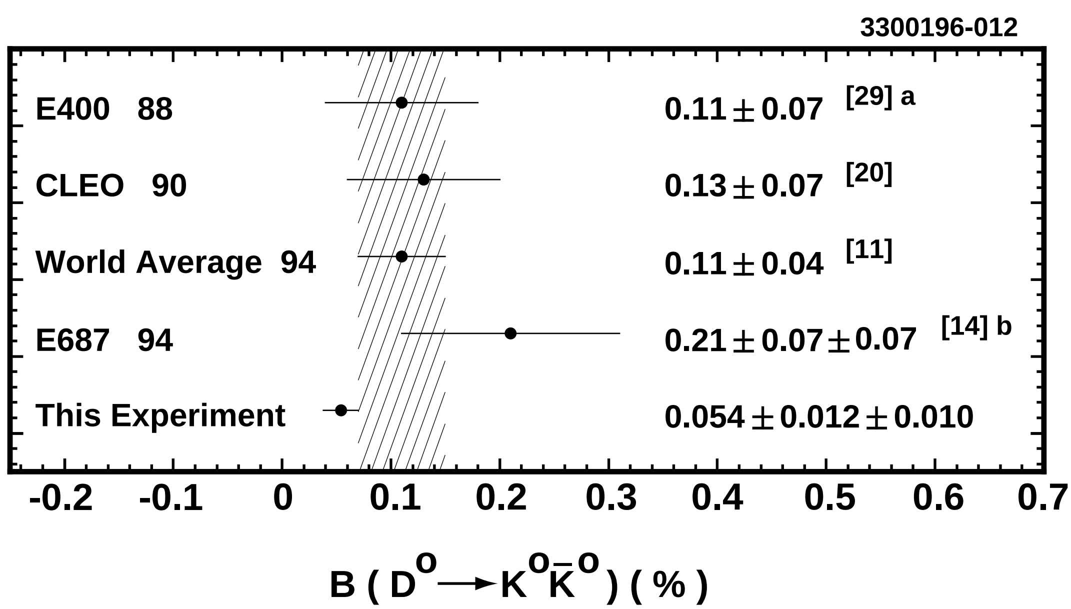


FIG. 12. The previous measurements and our result for the $B(D^0 \to K^0\bar{K}^0)$ channel. The hatched area indicates the world average. $^a$ We have used $B(D^0 \to K^+K^-) = (0.454 \pm 0.029)\%$ [11]. $^b$ We have used $B(D^0 \to \bar{K}^0\pi^+\pi^-) = (5.3 \pm 0.6)\%$ [11].

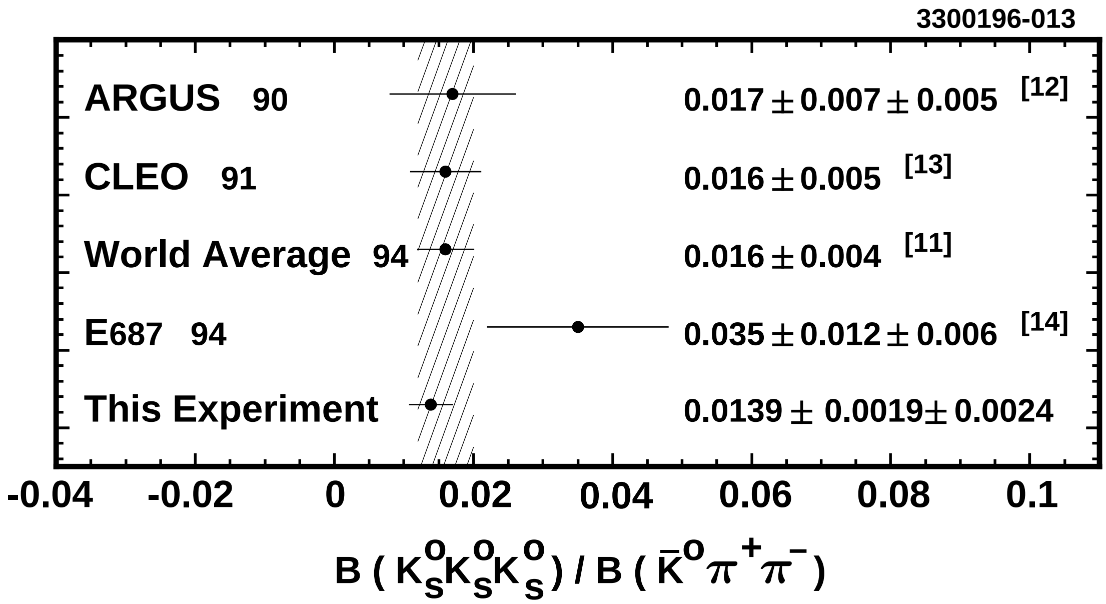


FIG. 13. The previous measurements for $B(D^0 \to K_S^0 K_S^0 K_S^0)/B(D^0 \to \bar{K}^0\pi^+\pi^-)$ and our result for this ratio. The hatched area indicates the world average.

# TABLES

TABLE I. The present predictions for the $KK$ branching ratios.

| Theory models | Branching ratio(%) | |
|---|---|---|
| | $K^+K^-$ | $K^0\bar{K}^0$ |
| Spectator Model [8] | 0.14 | 0 |
| WSB Model [1] | 0.56 | – |
| CC Model [2] | 0.25±0.06 | 0 |
| FSI Model [4] | 0.39 | 0.13 |
| I. Bigi [9] | 0.6 | – |
| QCD sum rule [5] | 0.3 | 0 |
| X. Y. Pham [10] | – | 0.3 |

TABLE II. Tags and normalization modes.

| Channel | Tag | Normalization mode |
|---|---|---|
| $K^+K^-$ | $D^{*\pm}$ | $K^-\pi^+$ |
| $K^0\bar{K}^0$ | $D^{*\pm}, D^{*0}$ | $\bar{K}^0\pi^+\pi^-$ |
| $K^0_SK^0_SK^0_S$ | No tag | $\bar{K}^0\pi^+\pi^-$ |
| $K^0_SK^0_S\pi^0$ | $D^{*\pm}$ | $\bar{K}^0\pi^+\pi^-$ |
| $K^+K^-\pi^0$ | $D^{*\pm}$ | $K^-\pi^+\pi^0$ |

TABLE III. Summary of systematic errors for the $K^0\bar{K}^0$ channel.

| | Systematic errors(%) | |
|---|---|---|
| Source of error | $D^{*\pm}$ tag | $D^{*0}$ tag |
| Uncorrelated error | 18.2 | 15.6 |
| Signal yield (cuts) | (17.4) | (12.5) |
| Non-resonant $\pi^+\pi^-$ background | (3.8) | (0.0) |
| MC statistics | (3.5) | (9.4) |
| Correlated error | 5.0 | 5.0 |
| $K^0_S$'s finding efficiency | (5.0) | (5.0) |
| Total | 18.9 | 16.4 |

TABLE IV. Summary of the branching fractions, where the first error is statistical and the second is the estimate of our systematic uncertainty.

| Channel | Theory(%) | $B$(%) | World Average(%) |
|---|---|---|---|
| $K^+K^-$ | 0.14∼0.6 | $0.454 \pm 0.028 \pm 0.035$ | $0.454 \pm 0.029$ |
| $K^0\bar{K}^0$ | 0∼0.3 | $0.054 \pm 0.012 \pm 0.010$ | $0.11 \pm 0.04$ |
| $K^0_SK^0_SK^0_S$ | | $0.074 \pm 0.010 \pm 0.015$ | $0.086 \pm 0.025$ |
| $K^0_SK^0_S\pi^0$ | | $< 0.059$ @90% CL | |
| $K^+K^-\pi^0$ | | $0.14 \pm 0.04$ | |